Photochemical evolution of palladium nanoparticles in Triton X-100 and its application as catalyst for degradation of acridine orange

Sudip Nath, Snigdhamayee Praharaj, Sudipa Panigrahi, Soumen Basu and Tarasankar Pal*

Department of Chemistry, Indian Institute of Technology, Kharagpur 721 302, India

A solution phase UV-photoactivation technique has been reported to prepare palladium nanoparticles. Aqueous H_2PdCl_4 solution was irradiated under UV-light (~365 nm, 340 lux) in a nonionic surfactant solution to produce Pd(0) nanoparticles. The particles generated in this method are stable, spherical and small (5–10 nm) with a tight size distribution. Catalytic activity of the photoproduced palladium nanoparticles has been substantiated through photodecolorization of aqueous acridine orange solution. It has been found that the photoproduced palladium nanoparticles have a profound influence on the reaction rate and the rate varies linearly with nanoparticle concentration.

Keywords: Catalyst, nanoparticle, palladium, Triton X-100, UV-irradiation.

RECENTLY, there is considerable interest on nanostructured transitional metal particles, because of their characteristic property, strikingly different from the bulk. Nanoparticles hold promise to employ them as innovative materials with new electronic, magnetic and thermal properties[1–3]. They have a large surface-to-volume ratio and consequently exhibit increased surface activity compared to bulk material, which enables them to act as a good catalyst[4]. Recent experiments suggest that when metal particles become small in size, their redox properties differ from the bulk metal and they also change in the presence of adsorbed foreign ions[5]. Thus nanosize transition-metal particles have attracted attention from both fundamental and technological viewpoints because of quantum size effect, which is derived from the reduction of free electrons[6].

Among all the transition metals, palladium is of interest because of its high catalytic activity in several reactions, e.g. hydrogenation[7], Heck reaction[8], C–C bond formation reaction[9], Suzuki reaction[10], cyclization reaction[11], etc. Several reports have been published regarding the preparation of stable palladium nanoparticles. Among them are the sonochemical method[12], sonoelectrochemical method[13], microemulsion technique[14] and other methods[15,16]. However, the reproducible preparation of small, stable palladium nanoparticles with tight size distribution is of immense importance and still remains a challenging task.

We report here the synthesis of palladium nanoparticles from aqueous palladium(II) chloride solution in poly(oxyethylene) isooctyl phenyl ether (Triton X-100, TX-100) under UV-irradiation. The particles were characterized by UV–visible spectrophotometry and Transmission Electron Microscopic (TEM) studies. We have also addressed the catalytic behaviour of micelle-stabilized palladium nanoparticles from the effective photodecolorization of acridine orange as a model system without the use of any other reducing agent. There exist several reports of dye degradation[17,18], even from our group[19], exploiting different reagents and experimental conditions. However, this is a fruitful attempt where photoproduced palladium nanoparticles have been exploited as catalyst for dye decolorization in a clean photochemical way.

All the reagents used were of AR grade. Deionized water was used throughout to prepare the solutions. Palladium(II) chloride ($PdCl_2$) was purchased from Merck (Germany) and used as received. A buffer solution of pH 9.4 was prepared using 0.02 M $NaHCO_3$ and Na_2CO_3 solutions. The surfactant, poly(oxyethylene) isooctyl phenyl ether (TX-100), was purchased from Aldrich (USA). Acridine orange was received from Merck. The chemical structures of acridine orange and TX-100 are given in Scheme 1. Palladized charcoal (Aldrich) having 10% by weight was used as received.

The experimental solution was taken in a quartz cuvette of 1 cm path length and photo-irradiated in a photo-reactor fitted with germicidal lamps of wavelength ~365 nm (Philips, India). The photoreactor can produce a flux of 100–850 lux (1 lux is 1 lumen light/sq. cm/s). The flux was monitored using a digital lux meter (Model LX 101, Taiwan). Light intensity inside the photoreactor was calibrated with an Ophir power meter (NOVA display and 30-A-SH sensor). The number of photons absorbed by unit volume of sample per second from the photoreactor of 100 lux is 3.03×10^{15}. The average temperature inside the photoreactor was 30 ± 2°C. UV–visible spectra of each solution were measured in a Shimadzu UV-160 digital spectrophotometer (Kyoto, Japan) with a 1 cm quartz cuvette. Nanoparticles were characterized by TEM studies in a Hitachi H-9000

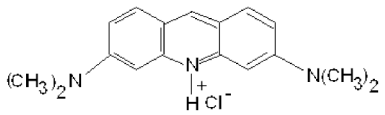

Acridine Orange

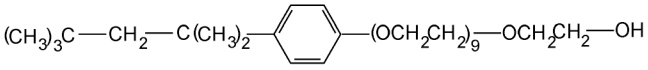

Triton X-100

Scheme 1.

*For correspondence. (e-mail: tpal@chem.iitkgp.ernet.in)

NAR Instrument (Japan) at a magnification of 100 k. The sample was prepared by placing a drop of solution on a carbon coated copper grid.

Accurately $PdCl_2$ 0.208 g was dissolved in 100 ml 5×10^{-1} M HCl to form H_2PdCl_4 (10^{-2} M) and used as stock solution. An aliquot of 100 µl of the aqueous H_2PdCl_4 solution was mixed with 3 ml of TX-100 (10^{-2} M) in a quartz cuvette and then the mixture was photoirradiated for 30 min with a flux of 340 lux. Progress of the reaction was monitored spectrophotometrically at a regular interval of 5 min. Appearance of a faint black colour indicates the formation of palladium nanoparticles. To study dye degradation, an aqueous solution of the dye (3 ml, 10^{-4} M) and palladium nanoparticles (preformed; 100 µl, 3.2×10^{-4} M) was mixed together and the solution was irradiated with UV-light (340 lux) inside the photo-reactor. The successive decrease in absorbance of the reaction mixtures was monitored using the UV–visible spectrophotometer at the regular interval of 5 min.

Formation of Pd nanoparticles by both chemical and photochemical means is indicated by the appearance of faint black colour of the solution. Photoevolution of Pd particles with sizes in the nanometre regime was monitored spectrophotometrically following gradual development of the spectral profile in the range 200–700 nm (Figure 1). After complete reduction of Pd(II) ions in surfactant solution, there was no further change in the nature and profile of the spectrum. It is to be mentioned that the spectral profile of the reduction is different in the present scenario than that observed in wet chemical pathways. Previously it was reported[20] that the generation of palladium nanoparticles could be monitored spectrophotometrically by following the increase and decrease in absorbance values at ~ 400 and 250 nm respectively, where the method adopted was wet chemical. An aqueous solution of H_2PdCl_4 showed a shoulder at ~250 nm and a peak at ~400 nm. After the reduction generated Pd particles exhibited a featureless absorption profile in the range 300–500 nm (Figure 1).

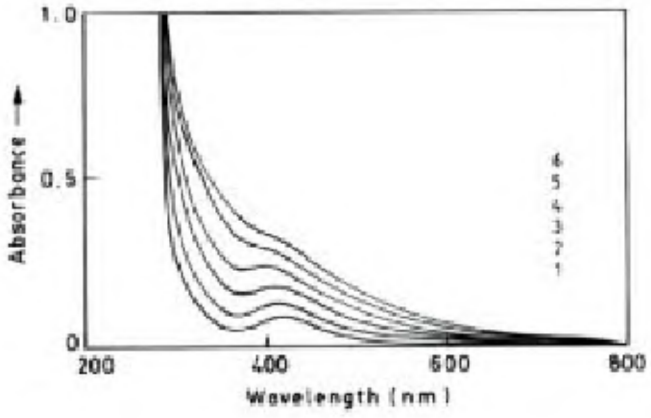

Figure 1. Absorption spectrum of photo-evolution of Pd(0) nanoparticles. Time interval between successive measurements is 5 min. Condition: $[PdCl_2] = 3.2 \times 10^{-4}$ M, [TX-100] = 10^{-2} M, flux of UV-light = 340 lux.

It has been mentioned that the progress of reduction of palladium(II) ions in solution is indicated by the increase in darkness of the solution. The exposure time for complete reduction of all the Pd(II) ions in TX-100 for the experimental volume (3 ml) and concentration (3.2×10^{-4} M) was 30 min under 340 lux. However, higher irradiation time did not affect the absorption profile. Complete reduction of Pd(II) ions in TX-100 solution was confirmed from the constancy of the absorbance values. Once the reduction of Pd(II) is complete, the particles remained stable in the micelle for months together.

Figure 2 *a* shows the TEM images of photoproduced palladium particles prepared in TX-100 micelles. From the TEM images it is observed that the particles are quite small, within the size range of 5–10 nm, spherical in shape with a modest dispersity and tight size distribution. The average size distribution of the particles is shown in Figure 2 *b*. The histogram of the particle diagram is obtained by analysing images from several regions of the grid shown in Figure 2 *a*.

TX-100 molecules in this reaction serve the purpose of a stabilizing agent and a reducing agent under UV-irradiation in aqueous solution. Surfactants not only impart stability to the metal clusters but also control the size and shape of the nanoparticles. It has been described that a surfactant having an alcoholic group homogeneously reduces Au(III) without increasing the local concentration of the added reagents[21]. The same procedure has been adopted here to prepare Pd particles where the –OH group of TX-100 reduces Pd(II) in solution and also stabilizes the evolved particles.

Interestingly, when the mixture of H_2PdCl_4 and TX-100 micelle was kept in the dark for several days, there was no sign of evolution of Pd(0). The peak due to H_2PdCl_4 remained unaltered for a long time. The evolution was not also observed when the reactants were heated on a water bath for more than 1 h. In H_2O, 2-propanol, glycerol and PVA media, no generation of Pd particles was noticed either on UV irradiation or heating. All these facts speak for the essentiality of TX-100 as a reducing agent in the reaction.

The aqueous solution of H_2PdCl_4 upon UV-irradiation in TX-100 micelle produces Pd(0). Previously it has been mentioned that either UV-irradiation or heating could not produce palladium particles in H_2O, 2-propanol, glycerol and PVA media. This happens possibly because the hydrated electrons produced in these methods may not be able to reduce Pd(II) ions. Keeping these observations in mind the mechanism of particle formation has been formulated as follows. The Pd(II) species is reduced by hydroxymethyl radical generated by photolysis of TX-100 [*R*–O–CH_2CH_2OH, where *R* = $(CH_3)_3CCH_2C(CH_3)_2C_6H_4(OCH_2CH_2)_{\sim 9}$–] and the primary hydroxyl function (–CH_2OH) of TX-100 is oxidized to the carboxylate group (–COOH) which has been authenticated from IR spectra[22]. Initially nuclei are formed in the solution with homogeneous distribution. Then they tend to aggregate to form bigger particles

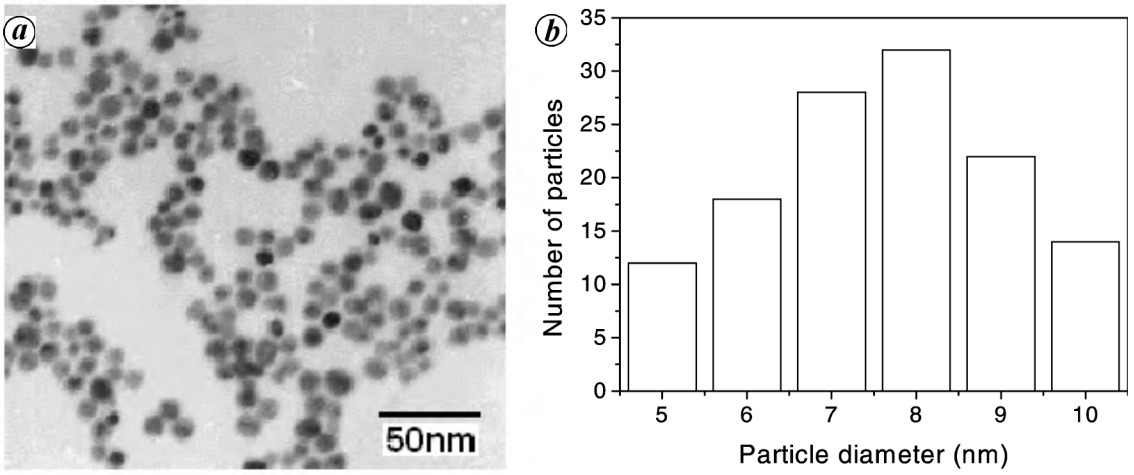

Figure 2. TEM images (*a*) and diameter histogram (*b*) of palladium nanoparticles.

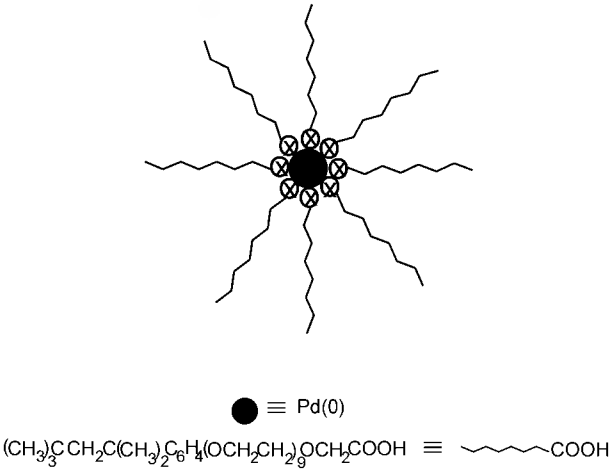

Scheme 2.

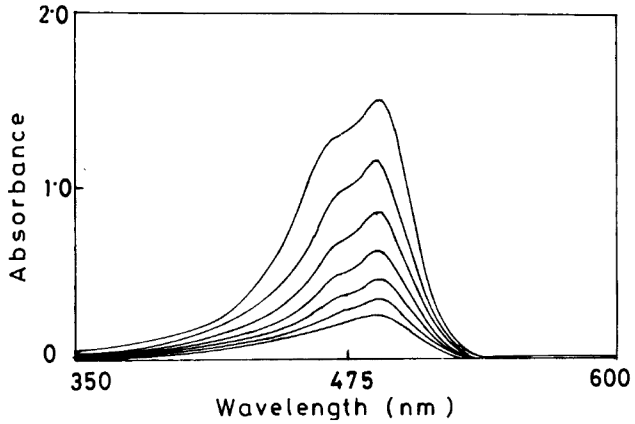

Figure 3. UV–visible spectra for photodegradation of acridine orange in water. The time interval between successive measurements is 5 min. Condition: [Dye] = 10^{-4} M, [Pd(0)] = 1.1×10^{-5} M, flux of UV-light = 340 lux.

and/or the remaining ions in the bulk get adsorbed on the surface of already formed particles. Now successive reduction of the adsorbed Pd(II) ions onto the preformed Pd(0) surfaces takes place auto-catalytically[23]. Addition of preformed Pd(0) particles accelerated the rate of formation of Pd(0) particles. The surfactant molecules render inhibition to this aggregation/association through the capping effect and thus act as particle stabilizers (Scheme 2). The hydroxymethyl functionalities of the surfactant molecules anchor the molecule at the cluster surface, while the hydrophobic chain protects the cluster from aggregation with the next neighbour due to electrostatic repulsion and steric hindrance, and thus inhibit coalescence[24–26].

To study the catalytic activity of the photoproduced palladium nanoparticles acridine orange was chosen as a model compound, which is photodecolorized under UV. Selection of the dye is based on the fact that the dye has different colour shades in its degraded and undegraded forms. To study the photodegradation process, aqueous solution of acridine orange was employed along with TX-100-stabilized Pd nanoparticles for UV-irradiation. Progress of dye degradation was monitored by the decrease in absorbance of the peak due to acridine orange at 489 nm. In Figure 3 the absorption spectra of successive decolorization of the acridine orange is shown. In the absence of Pd under the same experimental condition, a slow rate of photodecolorization was observed (Figure 4) in the experimental timescale. It is, therefore, obvious that palladium catalyses the reaction to a great extent. The dye becomes adsorbed on the surface of the metal nanoparticle and eventually decolorizes irreversibly. Palladium nanoparticles help in photodegradation of AO under UV irradiation. Again, the same dye reduction was studied in the presence of an equivalent amount of Pd-C in lieu of the photoproduced Pd. In this case insignificant dye degradation was observed (comparable to the uncatalysed degradation). In the photochemical process carbon particles on Pd inhibit not only the penetration of the dye towards the carbon-coated Pd particles, but also obstruct the passage of UV-light. Hence the rate of decolorization of the dye in the presence of Pd-C becomes

slow. This observation clearly vouches the catalytic effect of the nanosize Pd particles in the reaction. It is to be mentioned that the reaction could not be carried out in the presence of naked Pd due to aggregation and subsequent precipitation. It has been shown that decolorization of the dye depends linearly on the concentration of the catalyst particles used. Linear variation in the rate with the change in concentration of nanoparticles in the reaction mixture is shown in Figure 5. Interestingly, the rate of decolorization has been found to have a bearing on the flux of UV-light. Thus a detailed study has been carried out for dye reduction with variable flux of UV-light, keeping all other parameters unaltered. Figure 6 depicts a series of results where the absorbance values have been presented as a function of time with respect to different fluxes of UV-light.

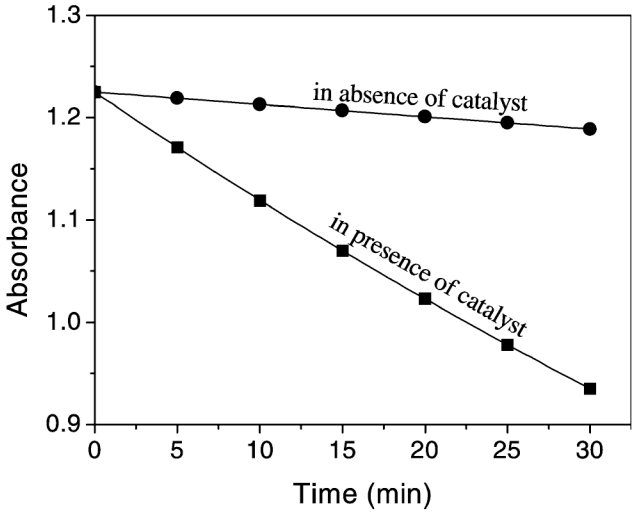

Figure 4. Absorbance as a function of time in absence and presence of catalyst. Condition: [Dye] = 10^{-4} M, [Pd(0)] = 1.1×10^{-5} M, flux of UV-light = 340 lux.

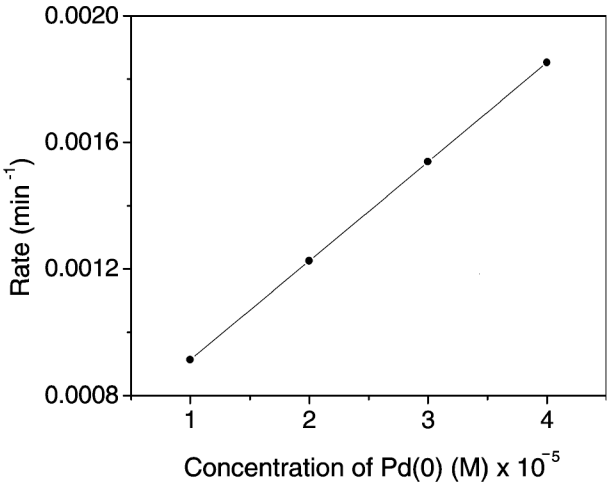

Figure 5. Variation of rate with different concentrations of Pd(0) in aqueous medium. Condition: [Dye] = 10^{-4} M, flux of UV-light = 340 lux.

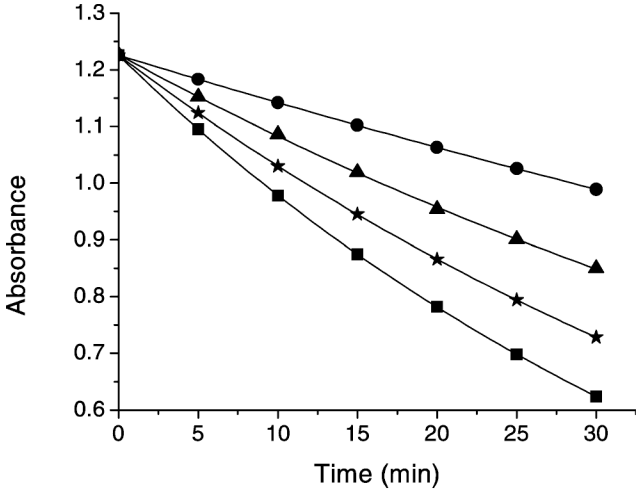

Figure 6. Absorbance vs time plot for photodegradation of acridine orange in the presence of TX-100 stabilized palladium nanoparticle in aqueous medium with variable flux of UV-light: ●, 120 lux; ▲, 340 lux; ★, 600 lux and ■, 850 lux. Condition: [Dye] = 10^{-4} M, [Pd(0)] = 1.2×10^{-5} M.

This communication discusses photochemical synthesis and stabilization of palladium nanoparticles in TX-100 micelle. The nonionic surfactant has been successfully employed as a reducing as well as stabilizing agent for this process. The characteristic catalytic behaviour of Pd nanoparticles is established by studying the decolorization of acridine orange in the presence of UV-irradiation. It has been authenticated from the study that nanoparticles have a tremendous influence on the reaction, and the rate of dye reduction varies linearly with nanoparticle concentration. The simple, reproducible and less time-consuming preparation of stable palladium nanoparticle with effective catalytic efficiency becomes the key aspect here.

1. Henglein, A., Physicochemical properties of small metal particles in solution: 'microelectrode' reactions, chemisorption, composite metal particles, and the atom-to-metal transition. *J. Phys. Chem.*, 1993, **97**, 5457–5471.
2. Kamat, P. V., Photochemistry on nonreactive and reactive (semiconductor) surfaces. *Chem. Rev.*, 1993, **93**, 267–300.
3. Link, S., Size and temperature dependence of the plasmon absorption of colloidal gold nanoparticles. *J. Phys. Chem. B*, 1999, **103**, 4212–4217.
4. Marcial, M. and Roser, P., Formation of carbon–carbon bonds under catalysis by transition-metal nanoparticles. *Acc. Chem. Res.*, 2003, **36**, 638–643.
5. Belloni, J., Mostafavi, M., Remita, H., Marignier, J. L. and Delcourt, M. O., Radiation-induced synthesis of mono- and multimetallic clusters and nanocolloids. *New J. Chem.*, 1998, **22**, 1239–1255.
6. Teranishi, T. and Miyake, M., Size control of palladium nanoparticles and their crystal structures. *Chem. Mater.*, 1998, **10**, 594–600.
7. Niu, Y., Yeung, L. K. and Crooks, R. M., Size-selective hydrogenation of olefines by dendrimer-encapsulated palladium nanoparticles. *J. Am. Chem. Soc.*, 2001, **123**, 6840–6846.

8. Yeung, L. K. and Crooks, R. M., Heck heterocoupling within a dendritic nanoreactor. *Nano Lett.*, 2001, **1**, 14–17.
9. Kogan, V., Aizenshtat, Z., Popovitz-Biro, R. and Neumann, R., Carbon–carbon and carbon–nitrogen coupling reactions catalyzed by palladium nanoparticles derived from a palladium substituted Keggin-type polyoxometalate. *Org. Lett.*, 2002, **4**, 3529–3532.
10. Li, Y., Boone, E. and El-Sayed, M. A., Size effects of PVP–Pd nanoparticles on the catalytic Suzuki reactions in aqueous solution. *Langmuir*, 2002, **18**, 4921–4925.
11. Larock, R. C., Hightower, T. R., Hasvold, L. A. and Peterson, K. P., Palladium(II)-catalyzed cyclization of olefinic tosylamides. *J. Org. Chem.*, 1996, **61**, 3584–3585.
12. Arul Dhas, N. and Gedanken, A., Sonochemical preparation and properties of nanostructured palladium metallic clusters. *J. Mater. Chem.*, 1998, **8**, 445–450.
13. Qiu, X., Xu, J., Zhu, J., Zhu, Je, Xu, S. and Chen, H., Controllable synthesis of palladium nanoparticles via a simple sonoelectrochemical method. *J. Mater. Res.*, 2003, **18**, 1399–1404.
14. Iida, M., Ohkawa, S., Er, H., Asaoka, N. and Yoshikawa, H., Formation of palladium(0) nanoparticles from a microemulsion system composed of bis(N-octylethylenediamine)palladium(II) chloride complex. *Chem. Lett.*, 2002, **10**, 1050–1051.
15. Lu, W., Wang, B., Wang, K., Wang, X. and Hou, J. G., Synthesis and characterization of crystalline and amorphous palladium nanoparticles. *Langmuir*, 2003, **19**, 5887–5891.
16. Shen, Y., Bi, L., Liu, B. and Dong, S., Simple preparation method of Pd nanoparticles on an Au electrode and its catalysis for dioxygen reduction. *New J. Chem.*, 2003, **27**, 938–941.
17. Lachheb, H., Puzenat, E., Houas, A., Ksibi, M., Elaloui, E., Guillard, C. and Herrmann, J., Photocatalytic degradation of various types of dyes (Alizarin S, crocein orange G, methyl red, congo red, methylene blue) in water by UV-irradiated titania. *Appl. Catal. B: Environ.*, 2002, **39**, 75–90.
18. Roessler, A. and Jin, X., State of the art technologies and new electrochemical methods for the reduction of vat dyes. *Dyes Pigm.*, 2003, **59**, 223–225.
19. Jana, N. R., Wang, Z. L. and Pal, T., Redox catalytic properties of palladium nanoparticles: Surfactant and electron donor–acceptor effects. *Langmuir*, 2000, **16**, 2457–2463.
20. Jana, N. R. and Pal, T., Redox catalytic property of still-growing and final palladium particles: A comparative study. *Langmuir*, 1999, **15**, 3458–3463.
21. Gachard, E., Remita, H., Khatouri, J., Keita, B., Nadjo, L. and Belloni, J., Radiation-induced and chemical formation of gold clusters. *New J. Chem.*, 1998, **11**, 1257–1265.
22. Pal, A., Photoinitiated gold sol generation in aqueous Triton X-100 and its analytical application for spectrophotometric determination of gold. *Talanta*, 1998, **46**, 583–587.
23. Mandal, M., Ghosh, S. K., Kundu, S., Esumi, K. and Pal, T., UV photoactivation for size and shape controlled synthesis and coalescence of gold nanoparticles in micelles. *Langmuir*, 2002, **18**, 7792–7797.
24. Mostafavi, M., Marignier, J. L., Amblard, J. and Belloni, J., Nucleation dynamics of silver aggregates. Simulation of photographic development processes. *Radiat. Phys. Chem.*, 1989, **34**, 605–617.
25. Khatouri, J., Ridard, J., Mostafavi, M., Amblard, J. and Belloni, J., Kinetics of cluster aggregation in competition with a chemical growth reaction. *Z. Phys. D*, 1995, **34**, 57–64.
26. Brust, M., Bethell, D., Kiely, C. J. and Schiffrin, D. J., Self-assembled gold nanoparticle thin films with nonmetallic optical and electronic properties. *Langmuir*, 1998, **14**, 5425–5429.

ACKNOWLEDGEMENTS. We thank UGC and CSIR, New Delhi, and IIT, Kharagpur for financial assistance.

Received 24 February 2006; revised accepted 17 August 2006

Inertial oscillation forced by the September 1997 cyclone in the Bay of Bengal

K. Jossia Joseph[1,*], A. N. Balchand[2], P. V. Hareeshkumar[3] and G. Rajesh[1]

[1]National Institute of Ocean Technology, Chennai 601 302, India
[2]Cochin University of Science and Technology, Cochin 682 016, India
[3]Naval Physical and Oceanographic Laboratory, Cochin 682 021, India

Time-series measurements from a moored data buoy located in the Bay of Bengal captured signals of inertial oscillation forced by the September 1997 cyclone. The progressive vector diagram showed mean northeastward current with well-defined clockwise circulation. Spectral analysis exhibited inertial peak at 0.67 cpd with blue shift and high rotary coefficient of –0.99, which signifies strong circular inertial oscillation. The wind and SST also exhibited spectral peak at inertial band (0.69 cpd) with higher blue shift. The inertial amplitude of 148.8 cm/s corresponding to a wind stress of 0.99 N/m^2 and spectral peak near the local inertial frequency (0.653 cpd) indicate that the transfer of momentum was high.

Keywords: Bay of Bengal, cyclone, inertial oscillation, spectral analysis, wind forcing.

INERTIAL oscillations are manifestations of unforced ocean dynamics and are generally observed after the passage of cyclones[1–6]. Webster[7] reported that inertial currents occur everywhere in the ocean at all depths, with velocities ranging from 10 to 80 cm/s. Inertial oscillations are the balance between the rate of change of velocity and the Coriolis force, and can exist only if their frequency exceeds the local Coriolis frequency[8]. Wind forcing is a major initiator of inertial oscillation[9–11] and duration of the wind compared with the inertial period is the most important factor that governs the amplitude of inertial oscillation[12]. The direction of the inertial current at the time of wind forcing is also important in determining the amplitude of inertial currents. Price *et al.*[4] reported the largest inertial amplitude of 1.7 m/s associated with hurricane *Gloria*. The amplitude varies depending on the strength of generating mechanisms and they decay due to friction when the forcing stops[13].

Reports of inertial oscillation generated by cyclone passage are fewer in the Indian seas due to scarcity of time-series data to resolve the inertial components. Saji *et al.*[5] reported inertial oscillations forced by the November 1995 cyclone in the Bay of Bengal (BoB) utilizing drifter buoy data. Some studies[14–16] have also reported inertial oscillation as one of the major contributors to the current structure under various meteorological conditions in the

*For correspondence. (e-mail: jossiaj@niot.res.in)